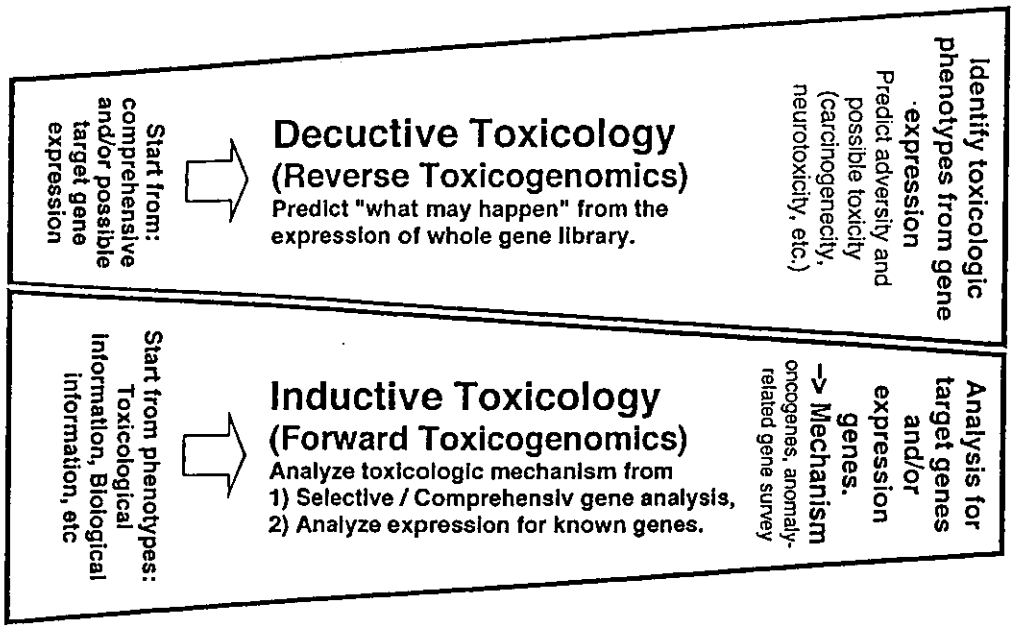

Fig. 24.1 Structures of inductive toxicology vs. deductive toxicology. The former begins its analyses from various toxicological phenotypes, including gross and/or pathological findings, and laboratory information, and proceeds toward the mechanism, whereas the latter focuses on predicting toxicological phenotypes solely on the basis of similarities in gene expression profiles without annotation of chemical characteristics. Nominally, the information on various phenotypes can be more diverse and far larger than the information on original gene expression profiling.

simpler technologies applying established expression profiles as new biomarkers, rather than sophisticated technologies requiring skills and experience. Since various phenotypes, including animal behaviour, are ultimately linked to the expression of genes and appear in consequence of the expression of a limited number of genes, much information can be condensed into a gene expression profile. At this moment, generalized reverse toxicogenomics is still a theory, except for the use of chips for customized purposes. However, the general applicability of species differences, including the extrapolation of responses from experimental animals to humans, the extrapolation of changes *in vitro* to responses *in vivo*, the possibility of analyzing multiple of toxicities from multiple toxicants, as well as the ability to extrapolate from high-dose markers to possible low-dose responses, and the discovery of early gene markers for long-term endpoints, are all promising future challenges [7].

In hematotoxicological applications, because the cellular targets of hematopoietic repertoires vary depending on the position of hierarchical structures along with their immaturity (that is, their 'stemness') and differentiation status, an accurate cell-separation technique for obtaining a reliable homogeneous fraction for relevant and repeatable comparison is necessary, such as flow-cytometric cell sorting with or without various markers for cellular identification or differentiation. Although it is generally accepted that such profiling differences are affected by sampling timing in various tissues in living animals, the hematopoietic tissue, as a continuously proliferating tissue, specifically shows a significantly different and labile profile in the micro-

array between the tissues immediately after damage and other tissues in the recovery phase. Furthermore, controversial time-sequenced responses differ between immature and differentiated cell compartments; thus, the timing of tissue sampling and the relevant comparison of fractionated blood cell compartments are critical for establishing a repeatable outcome [7].

In the following section, first, a brief overview of the physiological characteristics of hematopoietic stem/progenitor cells is given as a cellular biological basis of hematotoxicology. This is followed by a review of gene expression profiling, that is, molecular signatures, for stem cells. Two case studies on hematotoxicological toxicogenomics, involving radiation and benzene hematotoxicities, are then described so as to review two human ultimate leukemogens and their leukemogenic/hematotoxic profiling obtained by using a microarray. In the section on benzene exposure, gene expression profiling is specifically focused on in comparing p53 knockout (KO) and wild-type (WT) mice.

24.2
Hematopoietic Stem/Progenitor Cells in Hematotoxicology

Since the hematopoietic system consists of a mixture of heterogeneous cells with respect to not only functionally different cellular lineages, but also different stages in differentiation, an unfractionated blood sample may give differing gene expression profiles, and microarray data may not always provide an efficient and predictable outcome. As briefly described in the Introduction, specific attention should be paid to the preparation and interpretation of microarray data; thus, this section provides an overview of the hematopoietic system with respect to the nature of hematopoietic stem/progenitor cells and with special reference to microarray data processing and its interpretation.

The concept of a multipotent hematopoietic stem cell dates back to the radiation studies of Jacobson and coworkers in 1949–1950 [8–10], who observed autonomous hematopoietic recovery in lethally irradiated mice whose spleen or bone marrow had been shielded during otherwise lethal radiation exposure. In 1961, Till and McCulloch discovered that when normal bone marrow cells are transplanted into lethally irradiated mice, their spleens develop macroscopically visible colonies originating from regenerated hematopoietic cells and that the number of colonies directly correlates with the number of bone marrow cells injected, based on the hypothesis that each colony is derived from a single stem (termed spleen colony-forming unit, CFU-S) [11]. In 1965, they confirmed the clonogenic nature of CFU-S and then developed the currently used spleen colony assay for hematopoietic clonality [12]. Since Till and McCulloch's discovery, CFU-S was assumed to be the hematopoietic stem cells for more than 40 years; however, after the discovery of cells possessing a long-term repopulating ability in lethally irradiated mice, which were in addition found not to produce spleen colonies [13], CFU-Ss were renamed pluripotent hematopoietic progenitor cells, and the name of the cells in the common stem/progenitor cell compartment discussed here was changed to hematopoietic stem/progenitor cells.

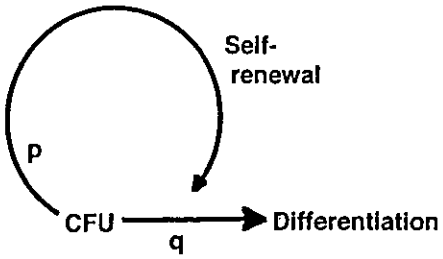

Fig. 24.2 Stem cell capability. Stem cells are capable of both proliferation (p) and differentiation (q), where p and q are independent variables; the ratio between the two is probabilistic. In the steady state, $p + q = 1$ [16].

Hematopoietic stem/progenitor cells, by definition, are targets of toxicological effects [14, 15]. Stem cells are capable of undergoing self-renewal (p) and/or differentiation (q), where p and q are independent variables. In the steady state, $p + q = 1$ (Figure 24.2) [16]. The progeny of hematopoietic stem/progenitor cells can be represented as a hierarchy of self-replicating, differentiating, and/or maturing daughter cells whose frequency depends on the relative probability of self-renewal during colony growth [16–19]. Relatively primitive hematopoietic stem cells, termed long-term repopulating stem cells (LTRCs), possess a relatively high capacity for multilineage differentiation and tend to generate mixed lymphomyeloid colonies in culture [18]. The mechanism of molecular switching of lineage-specific differentiation is not yet fully understood, but over-expression of TAL-1, a transcription factor involved in myeloid differentiation, inhibits lymphoid differentiation in ectopic over-expressing mice [20]. The mechanism of molecular switching was extensively studied by Lemischka's group [21] (see next section). The uncommitted hematopoietic progenitor cell, termed the *in vitro* colony-forming unit (CFU-C), can generate various lineage-specific colonies in semisolid culture, depending on the specific hematopoietic growth factors used to supplement the culture medium [16, 22].

Primitive stem cells and differentiating progenitor cells differ in kinetic characteristics. A method of evaluating stem cell kinetics *in vivo*, called the BUUV method, is available, and its use is introduced in Section 24.5.1. Once primitive stem cells (which tend to be predominantly in G_0) enter the cell cycle, they tend to proliferate at a more rapid rate than early progenitor cells [23]. Thus, elucidation of stemness is of special interest (see next section). One particular characteristic of the stem/progenitor function is explained by the significance of the activity of telomerase, a reverse transcriptase, as it is associated with the replicating potential of stem/progenitor cells. That is, primitive stem cells have a lower telomerase activity than do early progenitor cells, whereas early progenitor cells have high telomerase activity; however, as they mature or after repeated bone marrow transplantation, progenitor cells lose their telomerase activity [24, 25].

The shape of a hematopoietic colony growing in semisolid culture reflects its differentiation characteristics which, in turn, depend on the receptors expressed by its stem/progenitor cells and on the growth factor(s) used to supplement the culture medium (Figure 24.3). Colonies derived from immature stem cells are characterized by compactness, a high self-renewal capability, and a relatively low differentiation activity. Early uncommitted CFU-C generate an aggregation of several subcolonies called a mixed colony, indicating coexistence of a high self-renewal capacity and active differentiation ability. Although these colony-forming units in culture are

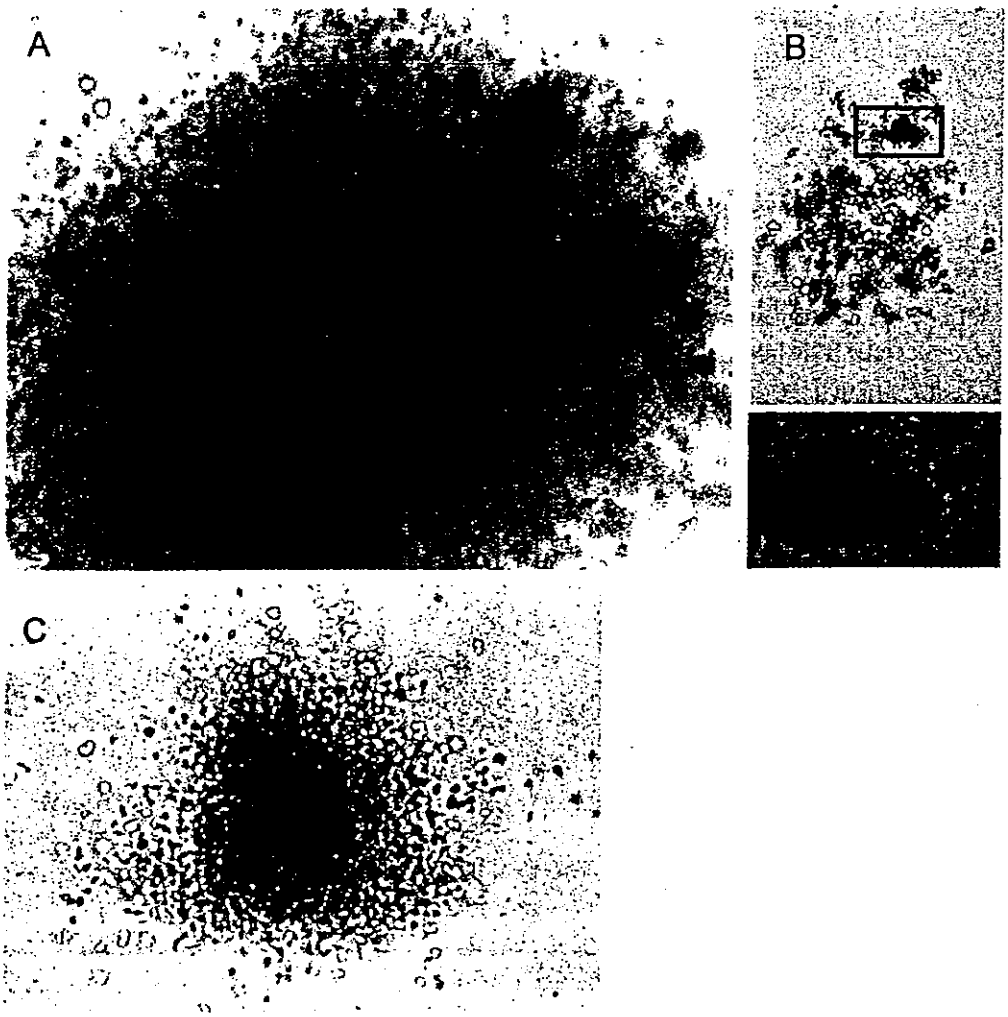

Fig. 24.3 Various hematopoietic colonies. Cultures of colonies were started from bone marrow cells, 2×10^4 cells mL^{-1}, grown in semisolid media with 0.8% methylcellulose in alpha MEM supplemented with 30% FCS (HyClone Lab.), 1% BSA, 10^{-4} M 2-mercaptoethanol, 1 μg mL^{-1} interleukin 3, and 2 U mL^{-1} erythropoietin. (A) Colony-forming unit with granulo–macrophage–megakaryocyte elements (original magnification, × 15); (B) burst colony-forming unit composed of erythroid elements (the inset at the bottom is a higher-magnification view of the boxed daughter aggregate at the top) (original magnification, × 15, top; and × 225 bottom); (C) colony-forming unit granulo–macrophage in the right (original magnification, × 15).

thought to be more differentiated progenitors than CFU-S, there are more primitive stem/progenitor cells, which are thought not to produce spleen colonies but which support the survival of lethally irradiated mice (LTRCs) [18, 26]). The hierarchy of the hematopoietic stem/progenitor cells mentioned above appears to express their own gene-expression profiling (see next section).

Correlating patterns of hematopoietic colony growth with changes in rates of hematopoietic stem/progenitor cell self-renewal and differentiation may be a useful tool for toxicological evaluation. That is, a large colony is derived from a progenitor cell whose

progeny has a high rate of both proliferation and differentiation, whereas an aggregate of numerous smaller colonies indicates derivation from a stem/progenitor cell with a high rate of self-renewal but a low rate of differentiation. Early stem/progenitor cells tend to generate compact colonies, whereas the more mature (committed) progenitor cells tend to produce dispersed colonies. The differentiation status may also reflect specific gene expression profiling (see next section). The shape and size of a hematopoietic colony can be an index of a stem/progenitor cell's kinetic status [23].

Current progress in the study of stem-cell plasticity is significant. The capability of stem cells to differentiate into various tissues is virtually unlimited. Not only have embryonic stem cells been shown to be able to differentiate into hematopoietic stem cells [27] or neuronal stem cells [28] and adipocytes [29], but hematopoietic stem cells have also been shown to be able to differentiate into hepatic oval cells [30] and hemangioendothelial cells [31]. Moreover, bone marrow stromal cells appear to be capable of differentiating into neuronal stem cells [32], hematopoietic stem cells [33], and cardiac muscle cells [34]. Such transorganic tissue stem cell systems may express common gene profiling on one hand, but each tissue stem cell system, including embryonic stem cells, expresses its own specific gene profiling [35] (see next section).

24.3
Molecular Signature of Stemness of Hematopoietic Stem/Progenies

Hematopoietic tissue consists of various blood cells and stromal cells, which form the hierarchy of the blood family. The proliferation and differentiation of blood cells are regulated by the interaction between blood cells, between blood cells and stromal cells, and between stromal cells indirectly through various cytokine secretions. Various blood lineages originate from each progenitor, which are different from common hematopoietic stem cells. Importantly, each progenitor cell expresses different molecular signatures (gene profiles), which enable them to maintain their particular characteristics. In this section, some trials to determine such particular gene-expression profiling of physiological stem/progenitor cells are introduced.

To elucidate the molecular signatures of hematopoietic stem/progenitor cells, it is important to characterize each expression profile that is specifically linked to each cell compartment, which is fractionated into various groups of bone marrow cells along with their differentiation from stem cells through progenitor cells to terminally differentiated cells. Thus, before microarray analyses, obtaining the expression profile of the specific fraction of the hematopoietic compartment provides essential information useful in future microarray analysis. Lemischka and coworkers analyzed a genome-wide gene expression defining regulatory pathways in stem cells [35] (Figure 24.4A). They fractionated $Sca^{pos}AA4.1^{pos}Kit^{pos}Lin^{neg/lo}$ [21, 36] and obtained cells from the fraction. cDNA libraries were obtained by removing of the $AA4.1^{neg}$ fraction [21]. According to the report of Phillips et al. [21], 42% of the genes studied either exactly matched data in PubMed queries or were homologous to known protein sequences, 39% were found in a list of expression sequence tag (EST) homology, and 14% of the genes studied found no match. Based on the functions predicted

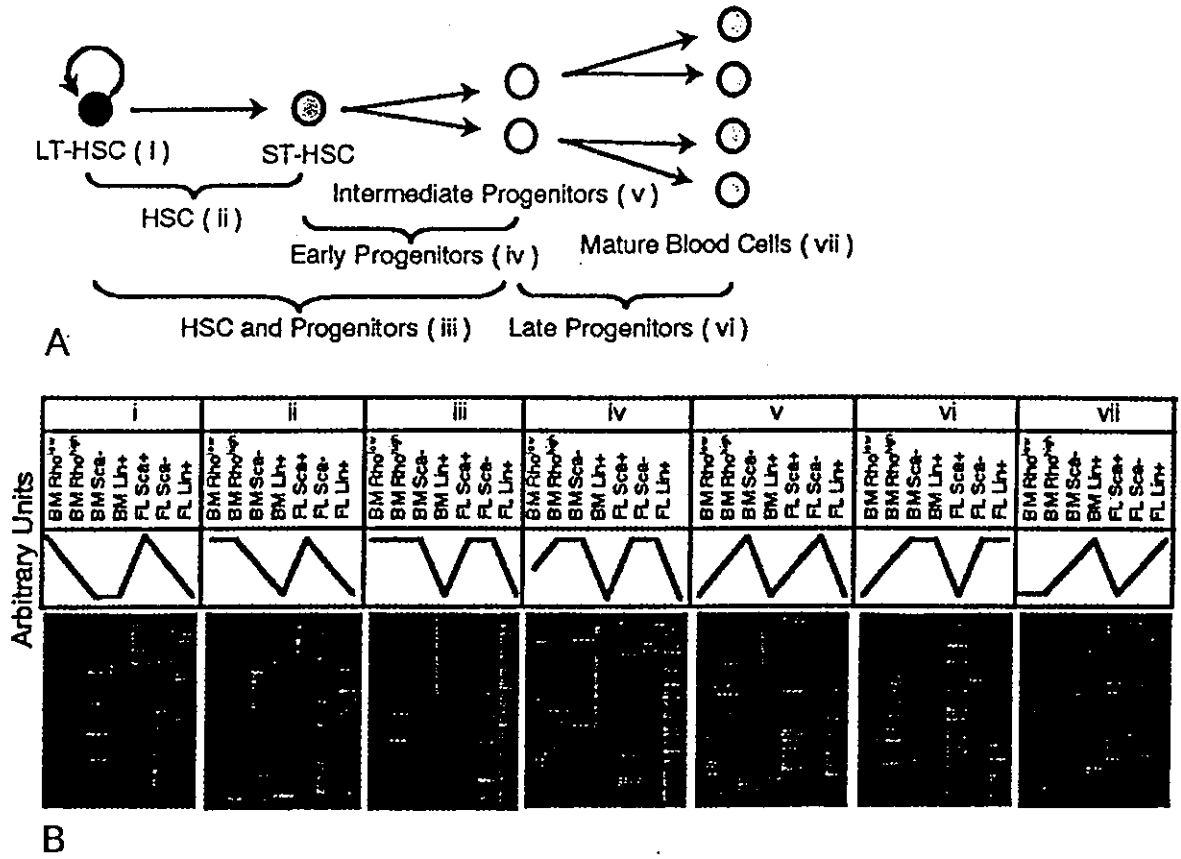

Fig. 24.4 (A) Hematopoietic hierarchy subgrouped into different stem and progenitor populations with their corresponding expression clusters (i to vii.). (B) Individual genes were assigned to expression clusters as described elsewhere, and relative expression levels are displayed in red (highest) to green (lowest) correlation. Predicted cellular roles of identified hematopoietic-specific gene products are shown [35]. (Reprinted with permission from Ivanova et al., *Science* 298: 601–604, 2002. Copyright 2002 AAAS.)

on the basis of the possible amino acid sequences mentioned above, the 39% EST consist of 32% genes for cell signalling, 24% for RNA synthesis, 18% for metabolism, 13% for protein synthesis, 7% for cell division, 4% for cell structure, and 2% for cell defence. The major functional categories of the entire subtracted genes consist of the following: five genes for transcription factors and chromatin-binding proteins (*ALL-1, AML-1/CBF, Dnmt-3b, Evi-1,* and *macroH2A 1.2*), with 10 novel related molecules; five genes for surface molecules (*Flk-2, Smoothened, Hem-1, CD34,* and *CD27*) with 10 novel related molecules; five genes for secreted proteins (angiopoietin, *IL-12 p35, MIP2, IL-16,* and MIP-related protein 2), with 10 novel non-annotated molecules; five genes for signalling molecules (*Dishevelled-1, Manic Fringe, Ski, DOKL, p56Dok-2*), with 10 novel related molecules; 10 genes homologous to *Caenorhabditis elegans* orthologs; and 10 genes homologous to *Drosophila* orthologs [21]. Recently, gene expression profiles for the stem cell fraction were directly observed [35]. On the basis of the expression profiles of the stem cell fraction separated by a cell

sorter ($Sca^{pos}AA4.1^{pos}Kit^{pos}Lin^{neg/lo}$), Ivanova and coworkers observed the microarray profiles of each bone marrow fraction separated into seven subgroups, from stem cell through progenitor cell to terminally differentiated cells, using cell-surface markers (Figure 24.4 B) [35]. According to information on the function of gene expression profiling specifically related to primitive hematopoietic stem/progenitor cells, the LT-HSC (long-term hemopoietic stem cells; $Sca^{pos}Kit^{pos}Rho^{low}Lin^{neg}$) fraction possesses two particular functions, transcription, such as *Hox* gene family, and cell-cell communication. The later consists of signalling ligands, receptors, extracellular matrix, and adhesion molecules, tends to be overexpressed in the HSC-specific gene set, and includes such LT-HSC–specific ligands as *Bmp8a*, *Wnt10A*, EGF family members *Ereg* and *Hegfl*, the angiogenesis-promoting factor *Agpt*, a ligand for the ROBO receptor family *Slit2*, and the ephrin receptor ligand *EfnB2*. The corresponding genes are recognized as involved in stem–stromal cell interactions in general, but *Wnt10A/Frizzled* and *Agpt/Tek* are, on the other hand, known to be expressed solely in stem cells. (Further, expression of these genes are also known to be common in the early development of embryonic stem cells.) In their reports [35], a large amount of supporting online materials and raw data including those for 4289 genes were attached, which were obtained by using Affymetrix systems (the above is excerpted with permission from NB Ivanova et al., *Science* 298: 601–604 (2002); copyright 2002 AAAS). Similar trials were performed by Park et al. [37], Ma et al. [38], and Attia et al. [39]; however, the data obtained cannot be compared among the reports, because the microarray systems and fractionation methods used were different. Also, overlapping genes were rarely observed because the stem cell compartments sorted out were different. Changes in the above-mentioned expression profiles diagnostic of stemness due to hematotoxicity are of special interest to analyze as a possible stem cell-specific response (see Sections 24.5.3, 24.5.5, and the Summary).

Interestingly, when gene expression was compared among embryonic, neuronal, and hematopoietic stem cells, 283 genes were commonly expressed in these three stem cell systems among the 2359 genes in the HSCs (Figure 24.5) [35]. Future mi-

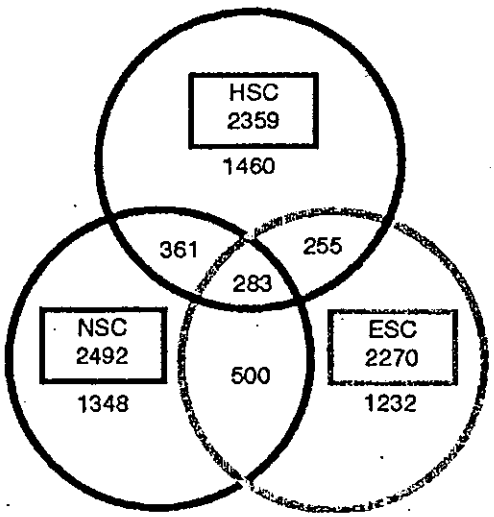

Fig. 24.5 Overlapping gene expressions in diverse murine stem cells. Venn diagram showing shared and distinct gene expressions among neuronal stem cells (NSCs), embryonic stem cells (ESCs), and hematopoietic stem cells (HSCs) [35]. (Reprinted with permission from Ivanova et al., *Science* 298: 601–604, 2002. Copyright 2002 AAAS.)

croarray studies on stem cells from different tissues and embryonic stem cells may elucidate the molecular mechanism underlying the plasticity of stem cell differentiation described in this section.

24.4
Radiation Hematotoxicity and Leukemogenesis

24.4.1
Radiation Effects on Hematopoietic Stem/Progenitor Cells

The idea that radiation can cause leukaemia was first raised in 1911 by von Jagie et al. [40], who described an increased incidence of leukaemia among clinical radiologists working with radiography and radioisotopes. This concept was reinforced by the high incidence of leukaemia among nuclear-bomb victims in Hiroshima and Nagasaki [41]. As indicated elsewhere, multiple hits are required for acute myeloid leukaemia (AML) to develop in this setting [41]. This suggests that younger individuals are potentially at greater risk of leukaemia because they have a greater risk for a secondary hit within their lifetime than do older individuals, although such a trend can be seen only when risks are broken down into age classes. In the setting of chronic myeloid leukaemia (CML), which presumably requires only a single hit or a few hits, younger individuals are also at higher risk than are older members of the general population [41].

The evolution of leukaemia from hematopoietic stem/progenitor cells has been well documented by a number of investigators [42–44]. Consequently, the incidence of radiation-induced leukaemia can be represented by a convex curve in which the incidence of leukaemia decreases at doses of radiation higher than 400 cGy [43], since high-dose radiation exposure does not induce leukaemia but instead causes excessive stem cell killing. If one takes into account stem cell survival after radiation, it is possible that the least number of stem cells is required for induction; thus, increased risk correlates with radiation dose [45]. One can calculate the actual risk by incorporating the total number of bone marrow stem/progenitor cells into the calculated survival curve for hematopoietic stem/progenitor cells (Figure 24.6A): The integral (shaded area) between the two lines corresponds to a high leukaemia risk. As the radiation dose approaches zero or exceeds 500 cGy, the respective integral areas increase or decrease, and the exponential risk approaches but never reaches zero, even with an infinite number of experimental subjects.

Interestingly, there are two settings in which the incidence of radiation leukaemia increases continuously with increasing radiation dose, namely, during fractionated radiation exposure and with p53 gene deficiency. With fractionated radiation exposure, using 100 divided doses, a different risk curve is obtained [45]. Using hematopoietic spleen colony assays, we found much flatter curves for both stem cell survival and leukaemia risk after single-dose radiation rather than after fractionated-dose radiation, even at high doses (Figure 24.6B). What type of gene expression profiles participates in these particular settings is of special interest (see next subsection).

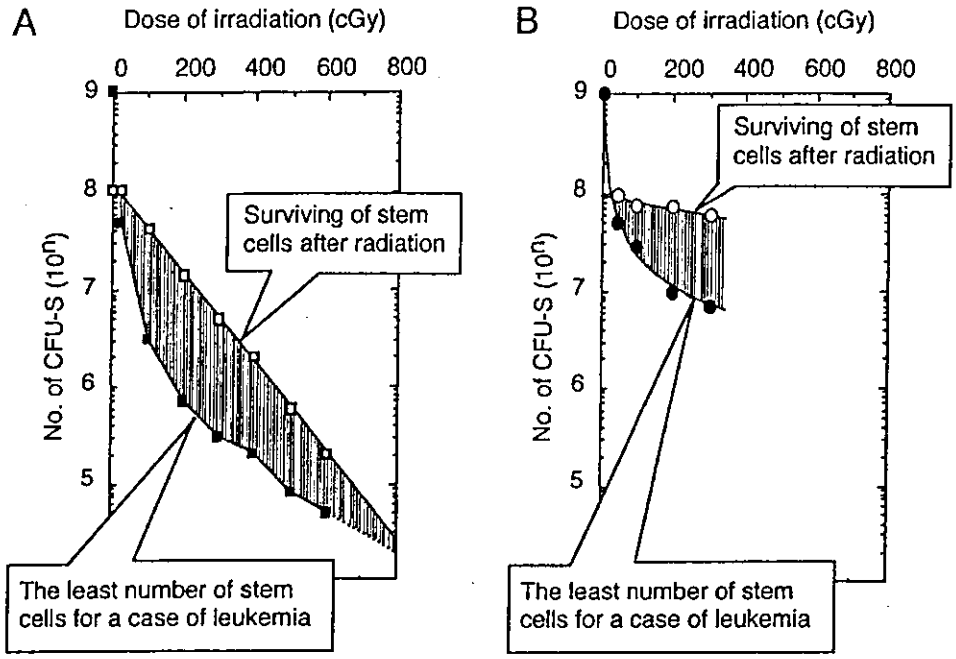

Fig. 24.6 Risk of radiation-induced leukaemia. Incidence of radiation-induced leukaemia and possible risk calculation represented by the shaded area between survival of stem cells (open symbols) and the fewest stem cells needed for a leukaemia case (closed symbols) as a function of radiation dose. (A) Single dose of radiation and (B) 100 split doses, were given [45].

Radiation induces apoptosis in mouse hematopoietic stem/progenitor cell compartments. Using p53-deficient (p53 KO) mice, we determined whether p53 deficiency blocks apoptosis. As expected, the stem/progenitor cell survival curves were flatter in p53 KO than in WT mice, demonstrating that p53 deficiency induces resistance to apoptosis and, consequently, a higher incidence of leukaemia [46]. (Comparative graph on radiation leukaemogenesis using p53 KO mice similar to Figure 24.6 is not shown.) The increased incidence of leukaemogenesis associated with p53 deficiency is consistent with the observation of increased leukaemogenesis at high radiation doses (for example, 500 cGy) in these animals [47].

Primitive stem cells require cytokines, the stem cell factor (SCF), and interleukin-3 (IL-3) to proliferate and generate hematopoietic colonies *in vitro* [48]. Moreover, we should note that primitive hematopoietic stem cells, but not more mature progenitor cells, express the growth-inhibitory signalling molecule, the tumour growth factor (TGF) beta receptor [49, 50]. TGF-beta does not increase the number of colonies generated in culture from WT stem/progenitor cells. Interestingly, such negative regulation of TGF-beta for primitive stem/progenitor cells fails when bone marrow cells are harvested from p53 KO [50]. It is also of interest that mice overexpressing the SV40-large T gene and made p53-deficient can suffer from a myelodysplastic syndrome, in which lack of regulation of growing potential in the primitive stem/progenitor cells is presumably induced by dysfunction of the negative regulator TGF-beta [51].

24.4.2
Radiation Exposure and Gene Expression Microarray

Irradiation of the hematopoietic system induces graded dose-dependent impairment of blood cells based on different radiation sensitivities at different stages of differentiation or with different positions in the cell cycle. Whereas common gene profiles among the doses were observed (40–50%), most of the genes did not overlap at different doses. To determine whether microarrays are useful for identifying these dose-related changes in gene expression, gene expressions at two doses, namely, 100 and 300 cGy, of gamma rays were compared with those in a nonirradiated control (Figure 24.7A). Although a possible common gene profile should be useful tool to search for biomarkers for dose–risk assessments, a unique gene profile at different irradiation doses should be useful for analyzing unique gene repertoires functioning at each radiation dose.

Among the genes expressed in the bone marrow one month after 100 or 300 cGy irradiation were those for *Mus musculus* p53-variant mRNA (U59758), cyclin G1 (L49507), cyclin-dependent kinase inhibitor 1C (*p57*; U22399), *M. musculus* mRNA for cyclin B1 for cell cycle (X64713), *M. musculus* apoptosis-inducing factor AIF mRNA (AF100927), *M. musculus* mRNA for caspase-12 for apoptosis-related genes

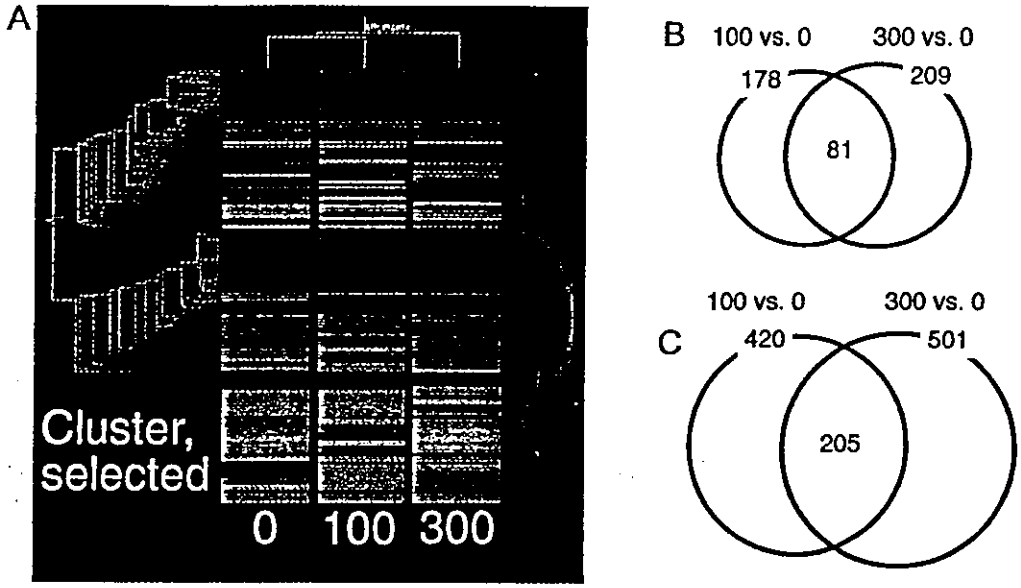

Fig. 24.7 (A) Cluster diagrams of gene trees, comparing the expression profiles among the groups (0, 100, and 300 cGy). GeneSpring software was used to normalize absolute gene expressions for each dose; the lowest expression level is shown in blue, the highest in red, and the intermediate in yellow. Most of expression profile patterns among the groups here seem to be similar in spectra, except in the region indicated by the green box, where the cluster regions selected show different expression profiles for each dose group, as shown on the bottom. (B) and (C) Venn diagrams showing (B) the numbers of genes expressed greater than twice the control levels and (C) the number of genes expressed less than half the control levels. The size of each circle is relative to the number of genes with changed expression, revealing that a larger number of genes was down-modulated (C) by irradiation, and one third of genes were up-regulated (B) by irradiation.

(Y13090), *M. musculus N-myc* gene, 3′ end and MoMuLV-like endogenous provirus, 5′ end (M29211), *Mago-nashi homolog*, a proliferation-associated *Drosophila* ortholog (AF035939) for proliferation-related genes, *M. musculus* thioredoxin mRNA (U85089), a nuclear gene encoding a mitochondrial protein, and *M. musculus* thioredoxin-related protein mRNA (AF052660) for oxidative-stress–related genes. Dose-related gene expression showed that many genes, that is, *M. musculus* endogenous retroviral sequence Mu ERV-*L gag, pol*, and dUTPase genes (Y12713), *M. musculus schlafen3* (Slfn3) mRNA (AF099974), and *Ul-M-BH0-ajy-d-09–0-Ul.s1 M. musculus* cDNA, 3′ end (A1853444), are potential common genes for indicating radiation exposure, and that the mouse germline IgH-chain gene (DJC region segment D-FL16.1; J00475) and *caspase-12* (Y13090) are dose-dependent gene markers. Whether expression of the genes Y12713, AF099974, and A1853444 is altered at much lower radiation doses is of interest for their use as possible gene markers for low-dose radiation (Figure 7 B and C).

The gene expression profiles in spontaneous and radiation-induced tumours differed, which is another interesting finding. Since C3H/He mice produce less than 1% of spontaneous myeloid leukemias, if spontaneous myeloid leukaemia tissue is obtained from such rare cases by the subtraction method, such a method would provide a specific gene profile difference between these types of tumours and would contribute a unique gene marker for identifying leukemias possibly induced by radiation.

24.5
Benzene-induced Hematotoxicity and Leukemogenesis

24.5.1
Benzene Exposure and Cell Cycle in Hematopoietic Stem/Progenitor Cells

The first report on leukaemia induced by benzene inhalation was made by Delore and Borgomano in 1928 [52] who described in a case of leukaemia in a French pharmacist. However, experimental induction of leukaemia by benzene exposure was not successful for more than half a century, until Snyder et al. and our group reported it over two decades ago [53–55]. Nevertheless, the mechanistic background of benzene-induced leukaemia remained an enigma until the peculiar benzene-induced cell kinetics of stem/progenitor cells was recently elucidated in our study, in which we demonstrated a marked, continuous oscillatory decrease in peripheral blood and bone marrow cellularities during and after benzene exposure [14], which epigenetically preceded and led to the development of leukaemia more than a year later.

The BUUV method[1)] enables the determination of stem/progenitor-cell–specific cellular kinetics [56], such as labelling rate, cycling fraction of clonogenic progenitor

1) The BUUV method involves incorporation of bromodeoxyuridine (BrdU) through an osmotic minipump, followed by specific purging of BrdU-containing cells by exposure to ultraviolet light at a specific wavelength, followed by assaying the ratio of hemopoietic colonies between the purged and the control. Hemopoietic stem/progenitor cell-specific parameters for cell kinetics, such as a doubling time, size of the cycling (i.e., DNA-synthesizing) or quiescent cell fractions, and also the size of cycling fraction per unit time-interval can be obtained (Figure 24.8A).

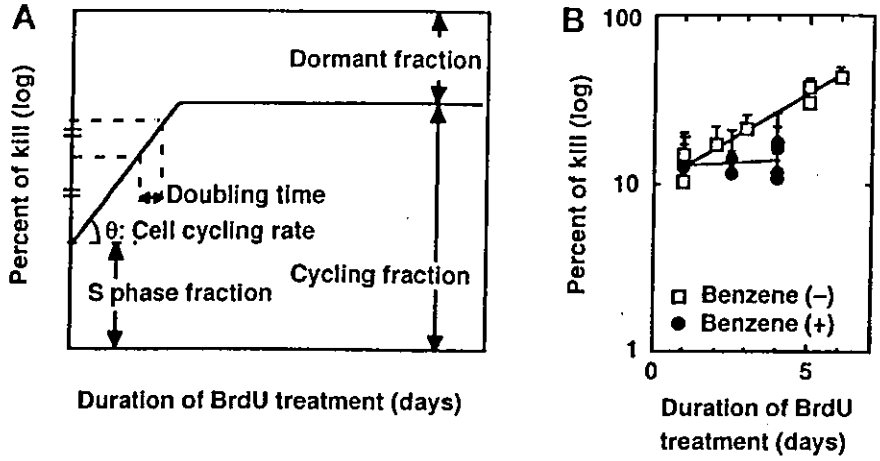

Fig. 24.8 (A) BUUV method of measuring cycling stem cells: model and parameters. Method for evaluating stem cell kinetics. Continuous infusion of bromodeoxyuridine via an osmotic minipump was used to label cycling cells, followed by UV exposure to kill the labelled cells. Then the surviving stem cells formed hematopoietic colonies [56]. (B) Cell cycle of granulo–macrophage colony-forming unit (CFU-GM) during exposure of normal mice to benzene. Note the significant suppression of the cell cycle fraction during benzene exposure with respect to the nonexposed control (closed circles and open squares, respectively).

cells, and other cell cycle parameters (Figure 24.8A). The cycling fraction of stem/progenitor cells was found not to undergo active haematopoiesis but rather to remain low in bromodeoxyuridine (BrdU) incorporation during benzene inhalation (Figure 24.8B). Furthermore, we found evidence that the decrease in the cycling fraction may be mediated in part by a slowing of stem/progenitor cell cycling per se or by p21 up-regulation [14].

Benzene-induced leukaemogenicity seem to differ between mice lacking p53 (p53 KO) and mice carrying WT p53. In p53 KO mice, DNA damage due to weak mutagenicity and/or chromosomal damage is retained, and those types of damage participate in the activation of protooncogenes and similar species, which leads cells to undergo further neoplastic changes. In contrast, in WT mice, a marked oscillatory change in the cell cycle of the stem cell compartment seems to be an important factor for these mice to experience a possible consequent mutagenic event.

Another interesting observation was the controversial experimental data concerning the level of actively cycling hematopoietic cells after benzene exposure. Although many investigators observed suppression of peripheral blood and bone marrow cellularities, some observed a suppression of cell cycling in the bone marrow, as measured by a decrease in tritiated thymidine incorporation [57], whereas others observed a marked increase in the number of cycling stem/progenitor cells in bone marrow and peripheral blood [55, 58, 59]. Careful analysis of these apparently conflicting data revealed increased cell cycling occurring at least two hours after the termination of benzene exposure. Thus, the higher tritiated thymidine incorporation documented by Cronkite et al. [55] 18 hours after the termination of benzene exposure probably reflected a recovery phase.

Based on the above-mentioned findings, we initiated a series of studies in 1997 to elucidate the leukaemogenic effect of benzene in mice. Using the p53 KO mouse, we confirmed that benzene has a moderate genotoxic effect, as measured by a micronucleus test performed four weeks after the initiation of benzene inhalation. Moreover, p53-deficient mice manifested increased susceptibility to benzene-induced leukaemogenicity [60]. Similar findings regarding increased leukaemogenicity after benzene exposure have been documented by French et al. at the National Institute of Environmental Health Sciences [61]. Presumably, benzene-induced leukaemia was not detected in earlier animal studies because its manifestations was masked by either pancytopenia due to severe myelosuppression or by the use of a benzene dose too low to induce pancytopenia and/or leukaemia.

24.5.2 Gene-expression Profile after Benzene Exposure in WT Mice

Based on the background of benzene-induced hematotoxicity and its leukaemogenesis, the cDNA microarray analysis was focused on to determine whether it can elucidate the underlying mechanism. The results of cDNA microarray analysis showed a broad consensus that the p53 tumour-suppressor gene is central to the mechanism of action of benzene, by strictly regulating specific genes involved in the pathways of cell cycle arrest, apoptosis, and DNA repair. Such a close association of p53 gene function and benzene toxicity raises the question regarding the fate of mice whose p53 gene was knocked out after benzene exposure; thus, cDNA microarray analysis data from p53 KO and WT mice were analyzed with Genespring software. In p53 WT mice, the expression profiles of genes encoding many proteins involved in benzene metabolism (CYP2E1 [62] and myeloperoxidase (MPO) [63]), cell cycle or cell proliferation (p53, $p21^{waf1}$, cyclin G1, and Gadd45 [64]), and apoptosis (Bax-alpha [64]) were generally consistent with the cDNA microarray data for C57BL/6 mice described elsewhere (Table 24.1). A difference was noted in the expression patterns of specific genes taken during and after exposure of C57BL/6 mice to 300 ppm benzene for two weeks, as determined using the Incyte GEM cDNA microarray system (Figure 24.9). Figure 24.9A

Tab. 24.1 Genes reported to be up-regulated after benzene inhalation.

Category	*Gene name*	*Reference*
Metabolic enzyme	CYP 2E1	62
	myeloperoxidase (MPO)	63
Cell cycle	p53	64
	p21 (waf 1)	64
	cyclin G	64
	Gadd 45	64
Apoptosis	Bax-alpha	64
Oncogene	c-fos	82

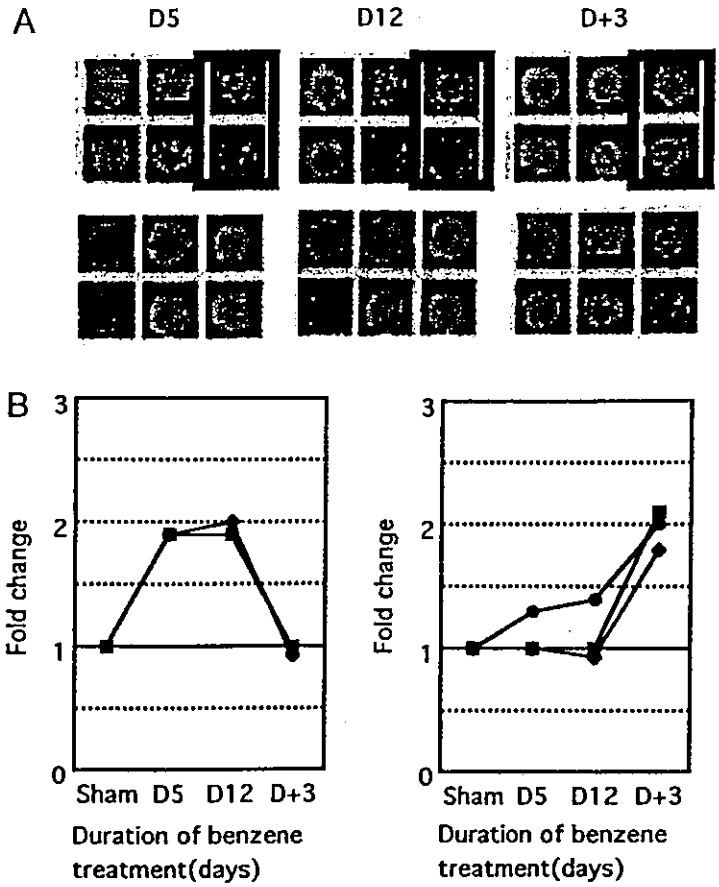

Fig. 24.9 Time course of microarray assays. Mice were exposed to benzene at 300 ppm for 1 week (D5) and 2 weeks (D12). D+3 designates the recovery group. The Incyte GEM system was used. Background-subtracted element signals were used to calculate the Cy3:Cy5 ratio. (A) Colour images of selected genes (two spots on the top right in each group) up-regulated (relative to nonexposed control) during and after benzene inhalation in red, down-regulated expression in green, and unchanged expression in yellow. Note that *MPO* (GenBank accession number X15378) shows up-regulation during benzene exposure followed by immediate down-regulation after exposure. (B) Time sequence of changes in expression of two different gene sets. *Left panel:* Genes up-regulated during benzene exposure followed by immediate down-regulation after benzene exposure: *MPO* genes (GenBank accession numbers X15313 and X15378, the same genes as in (A); squares and diamonds, respectively). *Right panel:* Genes up-regulated, gradually or immediately, after benzene exposure, chiefly represented by genes for DNA repair and proliferation during the recovery phase; *MCLP* (squares), *cdc2* (diamonds), and *lipocalin 2* (circles).

shows that the expression of MPO increased during exposure to benzene (right top square consisting two spots at D5 and D12) and then decreased three days after the termination of benzene exposure (right top square consisting two spots at D+3). Figure 24.9B (left) shows graphic expression of fold changes in the expression of MPOs (X15313 based on the mRNA sequence and X15378 based on the genomic sequence) mentioned above. There are corresponding spots for D5, D12, and D+3, revealing various expression patterns along the time course. A particular expression of the aryl-hydrocarbon receptor (AhR) was stably observed; its expression and the relationship to

benzene exposure could not be specified; however, as we previously observed, sensitivity to benzene toxicity is innate in AhR KO mice, implying that AhR transmits this sensitivity to benzene toxicity [15].

Also, a number of genes not previously reported show specific expression profiles after benzene exposure. We discovered the following points associated with the mechanism of action of benzene [65]: (1) benzene induces DNA damage in cells in any phase of the cell cycle; (2) for G1–S cell cycle arrest, not only the p53-mediated pathway but also the pRb gene-mediated pathway is involved; (3) p53-mediated *caspase 11* activation, aside from p53-mediated *Bax* gene induction, might be an important pathway for cellular apoptosis after benzene exposure; (4) *p58*, elongation factor-1 delta and Wee1-kinase may participate in G2–M cell cycle arrest induced by benzene; (5) DNA repair genes such as *Rad51, Rad 54* and *topoisomerase III* are activated after benzene exposure (Clastogenesis-related *topo-II* depression was insignificant.).

24.5.3 Cell-cycle–related Genes in p53 KO and WT Mice

Mice lacking the p53 gene generally had expression patterns similar to those of WT mice for genes involved in benzene metabolism (CYP2E1 [62, 66] and MPO [63]) and haemopoiesis, suggesting that p53 KO mice are also affected by benzene exposure to a similar extent, as also proposed previously based on the high number of micronuclei in benzene-exposed p53-deficient mice [67] (Table 24.2; see lines for up- or down-regulated both simultaneously in p53 KO and WT). To elucidate the difference in expression between p53 KO and WT mice, clustering analysis was performed [65]. The genes expressed include cell cycle- and apoptosis-associated genes. Table 24.3 shows

Tab. 24.2 Gene expression changes during and after benzene inhalation in the presence or absence of p53 gene.

Change in gene expression after benzene inhalation		*Category*
WT	*p53 KO*	
No change	No change	No relationship
	Up-regulated Down-regulated	Levelled by WT p53 during/after the benzene inhalation.
Up-regulated	No change	Genes up-regulated during/after benzene inhalation.
	Up-regulated	Genes up-regulated during/after benzene inhalation without any correlation of the p53 gene.
	Down-regulated	Genes levelled and also up-regulated by WT p53 with some other genes during/after benzene inhalation.
Down-regulated	No change	Genes down-regulated during/after benzene inhalation.
	Up-regulated	Genes levelled and also down-regulated by WT p53 with some other genes during/after benzene inhalation.
	Down-regulated	Genes down-regulated during/after benzene inhalation without any correlation of the p53 gene.

Tab. 24.3 Major changes in gene expression profiles in wild-type (WT) and p53-knockout (KO) mice. Mice exposed to 300 ppm benzene for 6 h d^{-1}, 5 d wk^{-1}, for almost 2 weeks and killed on day 12.[a)]

Gene name or name of protein encoded by the gene	*Fold change*		*Accession number*
	WT	*KO*	
Aldehyde dehydrogenase 4	1.07	2.44	U14390
Apoptotic protease activating factor 1 (Apaf-1)	1.16	1.75	AF064071
Bax-alpha	1.20	1.21	L22472
Bcl-2 alpha	0.91	1.66	L31532
Calcyclin	1.08	1.89	X66449
Caspase-9	0.83	1.59	AB019600
Caspase-9S	0.84	2.26	AB019601
Caspase-11	2.49	1.22	Y13089
Caspase-12	0.86	0.18	Y13090
c-fos	1.57	0.94	V00727
Cyclin B1	0.85	1.48	X64713
Cyclin D1[b)]	0.44	(–)	M64403
Cyclin D3	0.83	1.20	M86186
cyclin G1	1.67	1.32	L49507
CYP2E1	2.13	1.72	X01026
Cyclin D-interacting myb-like protein (Dmp1)	2.01	2.81	U70017
Elongation factor 1[b)]	3.12	(–)	AF304351
Gadd 45[b)]	1.63	(–)	U00937
Glyceraldehyde-3-phosphate dehydrogenase	1.06	3.34	M32599
G protein-coupled receptor (GPCR/EB11)	0.01	0.97	L31580
JNK2	1.07	1.82	AB005664
KSR1, protein kinase related to Raf protein kinase	1.11	2.57	U43585
Lactate dehydrogenase 1 (LDH1)	1.13	2.34	AW123952
Lactate dehydrogenase 2 (LDH2)	0.97	1.72	X51905
Metallothionein 1	4.89	0.93	V00835
Metaxin2	0.95	1.55	AF053550
mLimk1, *Mus musculus* protein kinase	2.67	1.18	X86569
Mph1/Rae 28, polycomb binding protein	4.97	0.06	U63386
Myeloperoxidase (MPO)	1.68	1.49	X15378
p21[b)]	1.37	(–)	U09507
p53, variant mRNA	1.03	0.13	U59758
p58, protein kinase inhibitor (PKI)	1.55	0.81	U28423
PERK, ER resident kinase	0.81	1.63	AF076681
PI3K catalytic subunit p110 delta	2.36	0.18	U86587
RAB17, member of RAS oncogene family	2.42	1.53	X70804
Rad50	1.23	0.40	U66887
Rad51	0.72	0.08	AV311591
Rad54[b)]	1.50	(–)	AV311591
Siva, pro-apoptotic protein	0.88	1.62	AF033115
Smad6	1.36	1.92	AF010133
Serum inducible kinase (SNK)	1.68	1.02	M96163
Superoxide dismutase, Cu/Zn	1.19	1.63	M35725
Topoisomerase III[b)]	1.90	(–)	AB006074
Tuberous sclerosis 2 (Tsc-2)	2.00	1.25	U37775

Tab. 24.3 (continued)

Gene name or name of protein encoded by the gene	*Fold change*		*Accession number*
	WT	*KO*	
Wee-1 [b]	1.95	(–)	D30743
Wig-1, p53-inducible zinc finger protein	1.83	0.07	AF012923
WISP1	0.68	1.26	AF100777
WISP2	0.83	8.32	AF100778
Wnt-1/INT-1	1.72	1.23	M11943

a) The studies involved two to four animals and the data were obtained by using Affymetrix gene chips. Mice were killed on day 12 immediately after benzene exposure.
b) No data available for p53 KO mice.

major selected genes whose expression showed p53-dependent benzene-induced decrease or increase (gene for G protein-coupled receptor 1), or in which gene expression was abolished in p53 KO mice. Cyclin genes, such as *cyclin B1* and *cyclin D3*, were generally activated in p53 KO mice by benzene exposure; in contrast, cell-cycle suppressor genes, including the G2–M cycle checkpoint gene, *p58* [68], were up-regulated in WT mice. These findings are compatible with the idea that the hematopoietic cell cycle continues in p53 KO mice even during benzene exposure, whereas it is arrested due to alterations in the expression of cell-cycle checkpoint genes, particularly the p53 gene, in WT mice. Such information may be very important for understanding yet-unknown toxicity mechanisms of chemicals. It is important to note here that such conclusions may be drawn by carefully and simultaneously screening different expression patterns of many genes having interrelated functions, even genes that show only small changes in expression level (about 1.5 to 2 fold). Investigation of the expression of a limited number of genes generally may not provide an insight into the main mechanism of action of chemicals or clues about the particular role of each of the investigated genes involved in the mechanism. Toxicogenomics may have a strong advantage from that point of view, as is also well described in the literature [7].

Ivanova et al. listed 17 genes including three EST genes in the cell cycle regulators among the genes profiled as stemness indicators [35]. Among them, 12 genes were confirmed in the list of genes expressed in the steady-state bone marrow of our present study. The expression levels of these 12 genes were all nearly comparable to that of beta actins; that is, comparable to the percent of the 'stem cell' concentration.

Two cell cycle regulator genes, *Wee 1* (D30743; one of the 17 mentioned above [35]) and *Mph1/Rae28/Edr1* (U63386; a member of polycomb, classified as one of the chromatin regulator genes in the stemness profile [35]), were significantly expressed after benzene exposure and were identified as possible candidates of marker genes for benzene exposure. Whether these possible marker genes for benzene exposure represent a change in an expression profile of stemness or are genes expressed in new, reacting progenitor cells after benzene exposure is not known; however, a possible role of these two genes as marker genes for benzene exposure is of much interest.

24.5.4
Apoptosis-related Genes in p53 KO and WT Mice

The microarray analysis results of p53 KO mice reminded us of the important role of the p53 gene in the mechanism of action of benzene. The genes regulated by the p53 gene, including *p21* [64], *caspase 11* [69], *PIK3K* [70] and *cyclin G1* [71], were distinctly up-regulated in the benzene-exposed WT mice (Table 24.3). It is of great interest that *caspase 11* rather than *caspase 9* was highly expressed after benzene exposure, suggesting that the p53-mediated activation of *caspase 11* is an important signalling pathway for apoptosis of bone marrow cells triggered by benzene exposure. This novel observation associated with the benzene toxicity mechanism, together with down-modulation of *caspase 12*, was similarly addressed in a study of the mechanism of chronic obstructive urinary disturbances, in which p53 KO and p53 WT mice were used [69]. On the other hand, the up-regulation and down-modulation of genes associated with oxidative stress was shown in p53 KO mice, which suggests that benzene may have produced oxidative stress in these mice (Table 24.3) [65]. It is not clear why oxidative-stress–associated genes are activated in p53 KO mice but not in WT mice; this may reflect deregulation of the redox cycle due to the absence of the p53 gene and the consecutive counteractivation of antioxidant enzymes [72]. The genes encoding apoptotic protease activating factor 1 (*Apaf-1*) and metaxin and the *Siva* gene were also up-regulated in the benzene-exposed p53 KO mice [65]. The expression of these genes may suggest that pro-apoptotic conditions are induced by benzene exposure of p53 KO mice. It was, however, found that survival or anti-apoptosis genes such as *bcl-2*, *caspase 9S* (an endogenous dominant-negative form of *caspase-9* [73]), and *Smad6* (an antagonist of the TGF-beta signalling [74]) gene, were also activated in p53-KO mice (Table 24.3) [65]. The up-regulation of the gene for PERK (ER transmembrane protein kinase) in p53 KO mice [65] indicates a triggering of the unfolded protein response (UPR) signalling pathway, resulting in a loss of *cyclin D1* [75] (which was statistically less confident in the present data).

24.5.5
DNA-repair–related Genes in the p53 Gene Network

Despite the possible DNA damage in bone marrow cells from p53 KO mice, the DNA repair system is not likely to be functioning efficiently in these mice, since DNA repair genes that were actively functioning in the WT mice exposed to benzene were not activated but rather suppressed in the p53 KO mice [65]. In association with cell proliferation and apoptosis, high expression levels of the *tuberous sclerosis* gene (*Tsc-2*), a tumour-suppressor gene encoding tuberin, and the gene encoding metallothionein 1 were noted in the WT mice (Table 24.3), raising the possibility that these genes are regulated by p53. The association of metallothionein with p53 transcriptional activity was recently postulated after study of an *in vitro* system in which metallothionein acts as a potent chelator to remove zinc from p53, thereby modulating p53 transcriptional activity [76]. The *Tsc-2* gene was recently reported to regulate the insulin signalling pathway mediated by AKT/PKB for cell growth [77, 78]. It is

noteworthy that *Tsc-2* is a target gene of 2,3,5-tris(glutathione-*S*-y) hydroquinone, a metabolite of hydroquinone for renal cell transformation [79]. The high expression level of the *mph1* (rae28) gene in the WT mice (Table 24.3) [65] along with severe depression of bone marrow cells was interesting in association with the sustained activity of hematopoietic stem cells [80]. Furthermore, the *Wnt-1* signalling pathway was also likely to be activated by benzene exposure. Aberrant expression of downstream genes such as *WISP1* and *WISP2* did not occur in the WT mice, but such expression was evident in the p53 KO [65]. Since the Wnt-1 signalling pathway is reported to regulate the proliferation and survival of various types of stem cells, including B-lymphocytes [81], the activation of both the *mph1* and *Wnt-1* genes may be associated with the rapid recovery of suppressed bone marrow cellularity after termination of benzene exposure. Some upstream genes encoding p53, such as those encoding cyclin D-interacting myb-like protein (*Dmp1*) and *KSR1* (protein kinase related to *Raf*) in the p53 KO mice, compared with those of the corresponding experimental group of WT mice, were up-regulated to a similar extent or even strongly enhanced in their expression (Table 24.3) [65]. This is another indication of the role of the p53-mediated pathway in the mechanism of action of benzene associated with cell cycle regulation.

Finally, by analyzing gene expression profiles, one can elucidate the mechanisms underlying benzene hematotoxicity. The next step is to further analyze the fractionated stem cell compartment and compare the results with those reported by Ivanova et al. [35]. For example, *CYP2E1* is known to be constitutively expressed in the WT mice [62], which was confirmed in the present investigation (Table 24.3). Interestingly, *CYP2E1* gene expression is in the list of Ivanova et al. [35]. Since the list was established by subtraction of the expression of cells other than stem cells from the expression in stem cell compartment, the expression of the *CYP2E1* gene targeted by benzene toxicity is assumed to be an exact reflection of benzene-induced stemness toxicity.

24.6 Summary

Molecular biology has enabled the elucidation of biological subjects by two strategies, namely, inductive and deductive approaches. The progress in the mouse whole-genome sequencing project has enabled the elucidation of bilateral interrelationships between toxicological phenotypes related to particular toxicants and expression profiles of pertinent genes induced by exposure to toxicants [7]. Since all the phenotypes observed through various traditional toxicological tests should be eventually linked to gene expression profiles, translation between phenotypes and gene expression profiles provides a promising tool for predictive toxicology, despite some phenotypes being expressed due to various nongenomic signal transductions. In fact, many gene expression trials have been performed to provide adequate molecular biological information on the underlying mechanism of such phenotypes. In this chapter, hematotoxic gene expression profiles after a single dose of 300 cGy irradiation or

repeated inhalation of 300 ppm benzene for 6 h a day, 5 days a week, for 2 weeks were introduced as an inductive approach of toxicogenomics. Then, a couple of plausible genes were selected with respect to the 'stemness profile' and discussed as a deductive approach for possible hematotoxicological applications of toxicogenomics. We did not incorporate data on clinical diagnosis, responsiveness to treatment, nor prognosis in this chapter, but considerable predictability has been shown in such trials elsewhere [83, 84].

Two major unresolved questions that we may have to pay specific attention to at this time are how one can define a specific mechanistic interpretation of the expression profiles for each discontinuous independent parameter; and how one can define a possible predictability of gene expression profiles (for carcinogenicity, for example) not only for the chemical group for which data were compiled during establishment of a database, but also for a group for which data were not incorporated into the database, that is, unknown chemicals. These unknown subjects should be given focus in future trials in toxicogenomics.

Finally, we have to note that the application of toxicogenomics to hematotoxicology should eventually focus on changes in the expression profiles of the hematopoietic stem cell/progenitor compartment, although the presented case study did not fully focus on this issue. In the WT mice, up-regulation of the *p53* gene did not appear in two weeks after intermittent benzene exposure, but was weakly detected a month after 300 cGy irradiation. Up-regulation of *cyclin G1*, downstream of *p53*, was observed after both benzene inhalation and 300 cGy irradiation, implying that the up-regulation of *cyclin G1* may be a relevant reflection of prolonged DNA damage.

When benzene was administered, down-regulation of *caspase 12* and up-regulation of *cyclin B1* was seen only when *p53* was knocked out (these gene changes may be hidden by *p53* gene regulation in WT mice) [65]. Participation of the same gene repertoire as in benzene exposure is observed even in the WT mice one month after 300-cGy irradiation, suggesting that the result may reflect a possible *p53* dysfunction in these irradiated mice.

For the future, more precise comparison between common gene expressions in the expression profiles in hematopoietic stem/progenitor cells after radiation exposure and benzene inhalation and the expression of genes on the stemness list compiled by Ivanova et al. [35] may lead to a clearer understanding of a possible marker repertoire of stem/progenitor cells for general hematotoxicological responses.

Acknowledgements

The article is dedicated to the late Dr. Eugene P. Cronkite. Financial support was received from the Japan Health Sciences Foundation (Research on Health Sciences focusing on Drug Innovation, KH31034) and the fund from Nuclear Research of the MEXT, Japan.